

# MEASUREMENT OF INTEGRATED GRADIENT AND FIELD QUALITY ON THE FIRST Q2 MAGNETS FOR HL-LHC\*

L. Fiscarelli<sup>†</sup>, S. Izquierdo Bermudez, G. Deferne, F. Mangiarotti, M. Pentella, P. Rogacki, S. Russenschuck, E. Todesco, European Organization for Nuclear Research, Geneva, Switzerland

## Abstract

The Q2 insertion quadrupoles for the High Luminosity upgrade of the LHC are currently being produced and tested. The test of the first units provides valuable information about the field quality of superconducting accelerator magnets built from Nb<sub>3</sub>Sn coils. This paper presents the results of the magnetic measurements performed on the prototype and series magnets with emphasis on field quality and field repeatability. The stability of the integral gradient is analyzed in view of the final installation in the machine.

## INTRODUCTION

The High Luminosity upgrade of the LHC (HL-LHC) includes the installation of large-aperture high-gradient quadrupoles as new inner-triplet magnets in the two interaction regions of the CMS and ATLAS [1] experiments. The required gradient of 132.6 Tm<sup>-1</sup> in a 150-mm aperture for the triplet quadrupoles, dictated the use of Nb<sub>3</sub>Sn as superconducting material for the magnet coils [2].

The new Q2 cryomagnet is composed of an MQXFB quadrupole and an MCBXFB corrector, as shown in Figure 1. The list of the main specifications for the MQXFB magnet is given in Table 1 for nominal operation at a proton center-of-mass energy of 7 TeV [3].

After a campaign of short models and prototypes for the validation of the design and the evaluation of the powering [4–6] and magnetic performance [7], the first full-length magnets have been built and tested [8]. Full-size magnets are tested in the final cryo-assembly configuration before installation in the tunnel with the requirement of a complete magnetic characterization.

In this paper, we first introduce the strategy and instruments for magnetic tests at ambient and cryogenic temperatures. Then, we discuss the main results, focusing on the measurement of integrated gradient and field quality.

Table 1: Main Specifications for the MQXFB Quadrupole

Parameter	Unit	Value
Aperture diameter	mm	150
Operational temperature	K	1.9
Nominal current $I_{nom}$	A	16230
Nominal gradient	Tm <sup>-1</sup>	132.6
Integrated nominal gradient	T	948.1
Magnetic length	m	7.2

\* Work supported by the HL-LHC project

<sup>†</sup> lucio.fiscarelli@cern.ch

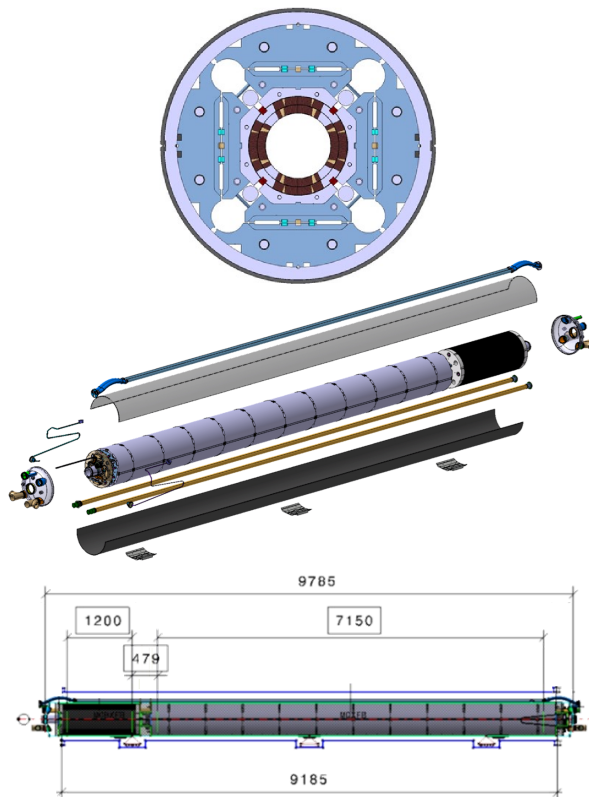


Figure 1: The cross-section of the MQXFB (top), an exploded view of the cold mass containing the main magnet MQXFB and the corrector MCBXFB (middle), the Q2 main dimensions in millimeters (bottom).

## FIELD MEASUREMENTS

In addition to the powering and training test, the Q2 magnets are characterized in terms of the transfer function of the integrated gradient, field quality, magnetic axis, and field direction. In this section, the strategy and the instruments for field measurements are described.

### Measurement Strategy

The magnetic measurements of the Q2 magnets have the following main objectives [9]: the quality control during the assembly process, the measurement of integrated gradient and field quality, the fiducial-markers localization for alignment, the collection of input data for the development of empirical magnetic-field models [10].

Since the magnetic measurement can be used as a diagnostic tool as well as to trigger actions for the fine-tuning of the field quality, the baseline is to measure the main field and harmonics at ambient temperature, on all the series magnets, at different phases of the magnet assembly [11, 12]: i) on the coil-pack assembly, ii) on the magnet full assembly before

loading, and iii) after loading. The results of these tests will be used to evaluate the need for magnetic shimming [13]. The magnetic axis and the field direction are also measured at ambient temperature after the finalization of the cold-mass assembly.

The integral gradient and harmonics are then measured at 1.9 K and at different current levels, with cycles as for the operation in the accelerator, to provide a complete magnetic characterization. In addition, the integral magnetic axis and integral magnetic angle are measured at operational conditions to allow the fiducial-marker localization for the alignment in the tunnel.

### Instruments

A number of accelerator projects have required the development of magnetic-measurement techniques by constantly improving the performance. The most relevant examples are the developments carried out for the SSC [14, 15], the RHIC [16], and LHC [17, 18] projects.

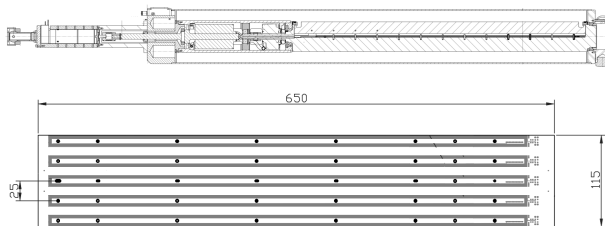


Figure 2: The rotating coil scanner used for the magnetic measurements at ambient temperature (top), and the PCB layout (bottom).

At ambient temperature, a longitudinal field scan using a short rotating-coil magnetometer [19] (Figure 2) provides a suitable characterization of the variation along the longitudinal magnet axis of the magnetic quantities of interest. The measurement accuracy of the field gradient by using a short rotating-coil magnetometer is limited by the knowledge of the coil surface and radius. Recent designs of coil magnetometers using PCB technology [20] have shown an improved relative accuracy at the level of a few units of  $10^{-4}$ .

Before installation in the accelerator tunnel, superconducting magnets are tested at cryogenic temperature up to nominal current and beyond. Due to the complexity of such a test and the typical schedule constraints, a magnetic measurement instrument must be easy to set up and able to reliably and accurately measure the total length of the magnet continuously during one or more powering cycles. A set of rotating-coil magnetometers, mechanically connected in series with the same motor/encoder unit, is called rotating-coil chain. The chain can have a length of several meters to cover the full length of the magnet, and to measure with a continuous rotation during hours of powering cycle. The rotating-coil chain used for the Q2 magnet has six equal modules. Each module has an overall length of about 1.4 m and is composed of i) a PCB board with the induction coils, ii)

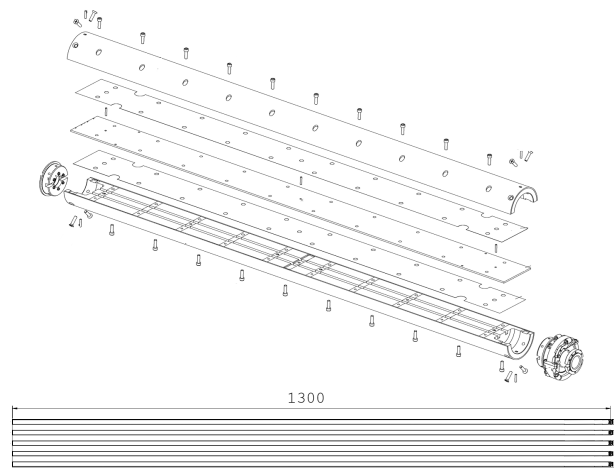


Figure 3: The 1.4-m-long module of the rotating coils chain (top) used for the magnetic measurements at cryogenic temperature: two composite shells hold a PCB plate (bottom) to form a cylindrical structure.

two half shells as support structure, and iii) the mechanical interfaces, see Figure 3.

An additional and complementary system is the single stretched wire: the most accurate instrument for the measurement of integral quantities such as integral gradient, field direction, and magnetic axis [21]. However, it does not provide any measurement of local quantities, and it is not well suited for measuring field harmonics, in particular at the different current levels of a typical excitation cycle. Therefore, the stretched wire is used, besides the determination of the magnetic axis, for a final measurement of the integrated gradient at cryogenic temperature and nominal current.

## MEASUREMENT RESULTS

At present time, three prototypes and four series MQXFB magnets have been built. The list of all tested magnets is shown in Table 2. In this section, the main results of magnetic measurements are presented and discussed. In particular, we will focus on the reproducibility and stability of the integrated gradient, and the field quality in terms of multipolar coefficients.

### Integrated Gradient

The transfer function – the ratio of the integral gradient and the excitation current – measured at ambient temperature by using the rotating coil scanner, and at nominal conditions by using the stretched wire, are reported in Table 2. The results show that the magnet-to-magnet reproducibility of the integrated gradient is within a range of 20 units of  $10^{-4}$  at ambient temperature, and within a range of 25 units at 1.9 K and nominal current. The production of the first magnets has not been homogeneous: i) a change of cross section was applied from the P2 [22], ii) the magnets P3 and 02 implement a series of modifications to address the performance limitations [23]. From magnets 03, all units are built with the same coil fabrication and assembly processes [24]. Therefore, we expect a more reproducible behavior.

Figure 4 shows the transfer function, measured with the rotating-coil chain, as a function of the current. The measurements show a spread of up to 50 units at intermediate currents due to the effect of the magnetic shims [25] that vary from magnet to magnet.

The results of a special measurement, performed as well with the rotating-coil chain during a plateau of 8 hours at nominal current, is shown in Figure 5. For the duration of the test, the integrated gradient remains stable within the measurement precision of  $\pm 2 \times 10^{-5}$ .

Table 2: Measurements of the Transfer Function of Three Prototypes and Four Series MQXFB Magnets

Magnet	Transfer function ( $\text{T kA}^{-1}$ )	
	Ambient temperature	$I_{nom}$ at 1.9 K
P1	63.394	58.562
P2	63.359	58.708
P3	63.328	58.616
O2	63.407	58.649
O3	63.458	58.571
O4	63.426	58.654
O5	63.434	–
Average	63.401	58.627
Range (units)	20	25

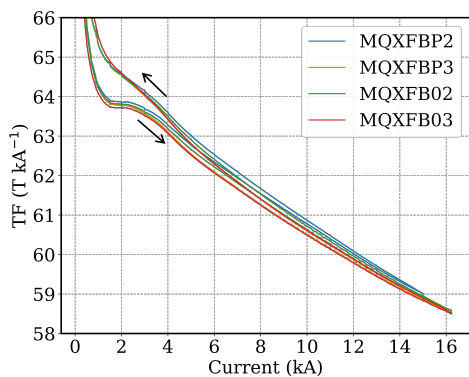


Figure 4: Transfer function (TF) measured as a function of the current on four different magnets. The arrows indicate the ramping direction.

### Field Quality

The multipoles, measured both at ambient temperature and 1.9 K expressed at the reference radius of 50 mm, are shown in Figure 6. All multipoles, at nominal conditions, are within the expected range of variation given by tolerances in the order of 30  $\mu\text{m}$  for the cable positioning. Some low-order multipoles, such as  $b_3$  on the magnet P2, the  $a_3$  on the magnet O2, or the  $a_4$  on the magnet O4, are corrected with the application of magnetic shims based on measurements at ambient temperature. The  $b_6$ , based on the measurement of the short models, has been corrected by tuning the coil geometry on magnets from the P2 [22].

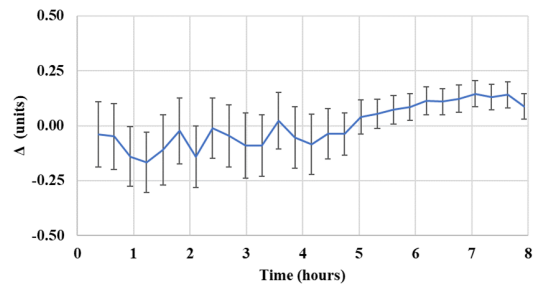


Figure 5: Stability of the integrated gradient measured with the rotating coil chain during a plateau of 8 hours at constant nominal current. Each point is an average of 100 measurements with the 3-sigma standard deviation as error bars.

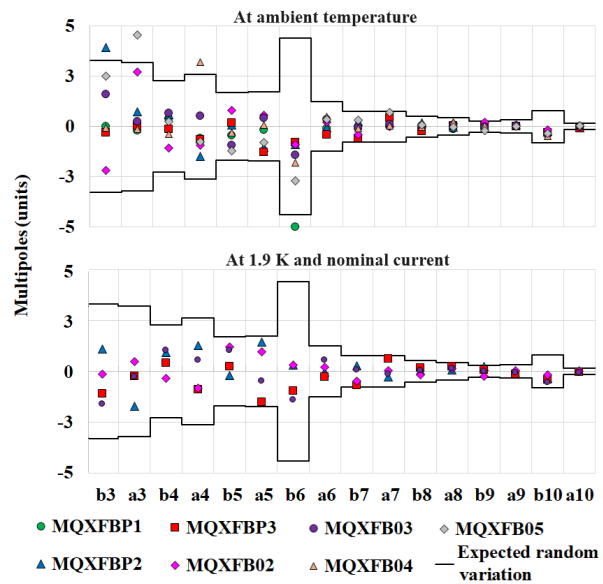


Figure 6: Integrated multipoles measured on the three prototypes and the first four series MQXFB quadrupoles. The solid lines show the expected range of random variation computed from random movements of 30  $\mu\text{m}$  of the conductor blocks in the coils. The reference radius is 50 mm.

## CONCLUSIONS

Three prototypes and four series Q2 magnets for HL-LHC have been built and tested. Specific instruments, together with a comprehensive strategy, have been developed for magnetic measurements both at ambient and cryogenic temperatures. The results of the magnetic characterization of seven magnets show that: i) the integrated gradient is reproducible from magnet to magnet within 20 units of  $10^{-4}$  and it is stable over long plateaus at nominal current within the measurement precision of  $2 \times 10^{-5}$ , ii) the field quality, after magnetic shimming, is under control and all multipoles are well within the acceptable range of variation.

## ACKNOWLEDGMENT

We gratefully acknowledge the work of the teams at CERN for both manufacturing and testing and the regular, open, and fruitful exchanges with AUP colleagues in the US.

## REFERENCES

- [1] G. Apollinari *et al.*, “High-Luminosity Large Hadron Collider (HL-LHC): Technical Design Report”, CERN, Geneva, Switzerland, CERN-2017-007, 2017.
- [2] P. Ferracin *et al.*, “Magnet design of the 150 mm aperture low- $\beta$  quadrupoles for the high luminosity LHC”, *IEEE Trans. Appl. Supercond.*, vol. 24, no. 3, Jun. 2014, Art. no. 4002306. doi:10.1109/TASC.2013.2284970
- [3] E. Todesco *et al.*, “The High Luminosity LHC interaction region magnets towards series production”, *Supercond. Sci. Technol.*, vol. 34, no. 5, p. 053001, 2021. doi:10.1088/1361-6668/abdba4
- [4] F. Mangiarotti *et al.*, “Test results of the CERN HL-LHC low-beta quadrupole short models MQXFS3c and MQXFS4”, *IEEE Trans. Appl. Supercond.* vol. 29, Art. no. 4001705. doi:10.1109/tasc.2019.2897229
- [5] G. Vallone *et al.*, “Summary of the mechanical performances of the 1.5 long models of the Nb3Sn low- $\beta$  quadrupole MQXF”, *IEEE Trans. Appl. Supercond.*, vol. 29, no. 5, pp. 1–5, Aug. 2019. doi:10.1109/tasc.2019.2898327
- [6] S. I. Bermudez *et al.*, “Performance of a MQXF Nb3Sn Quadrupole Magnet Under Different Stress Level”, *IEEE Trans. Appl. Supercond.*, vol. 32, no. 6, pp. 1–6, Sept. 2022, Art no. 4007106. doi:10.1109/TASC.2022.3167369
- [7] L. Fiscarelli *et al.*, “Magnetic Measurements on the First CERN-Built Models of the Insertion Quadrupole MQXF for HL-LHC”, *IEEE Trans. Appl. Supercond.*, vol. 28, no. 3, pp. 1–5, Apr. 2018. doi:10.1109/tasc.2017.2786684.
- [8] A. Milanese *et al.*, “Status of MQXFB quadrupole magnets for HL-LHC”, in *Proc. IPAC’23*, Venice, Italy, May 2023, pp. 3704–3707. doi:10.18429/JACoW-IPAC2023-WEPM060
- [9] E. Todesco and L. Fiscarelli, “Strategy for magnetic measurements for new HL-LHC magnets”, 8th HL-LHC Collaboration Meeting, CERN, Geneva, 15-18 October 2018. <https://indico.cern.ch/event/742082/>
- [10] N. Sammut, L. Bottura, and J. Micallef, “Mathematical formulation to predict the harmonics of the superconducting Large Hadron Collider magnets”, *Phys. Rev. Spec. Top. Accel Beams*, vol. 9, no. 1, Jan. 2006. doi:10.1103/physrevstab.9.012402
- [11] P. Ferracin *et al.*, “The HL-LHC Low- $\beta$  Quadrupole Magnet MQXF: From Short Models to Long Prototypes”, *IEEE Trans. Appl. Supercond.*, vol. 29, no. 5, pp. 1–9, Aug. 2019. doi:10.1109/tasc.2019.2895908
- [12] S. Izquierdo Bermudez *et al.*, “Progress in the Development of the Nb3Sn MQXFB Quadrupole for the HiLumi Upgrade of the LHC”, *IEEE Trans. Appl. Supercond.*, vol. 31, no. 5, pp. 1–7, Aug. 2021. doi:10.1109/tasc.2021.3061352
- [13] S. Izquierdo Bermudez *et al.*, “Second-Generation Coil Design of the Nb3Sn low- $\beta$  Quadrupole for the High Luminosity LHC”, *IEEE Trans. Appl. Supercond.*, vol. 26, no. 4, pp. 1–5, Jun. 2016. doi:10.1109/tasc.2016.2519002
- [14] G. Ganetis, J. Herrera, R. Hogue, J. Skaritka, P. Wanderer, and E. Willen, “Field Measuring Probe for SSC Magnets”, in *Proc. PAC’87*, Washington D.C., USA, Mar. 1987, pp. 1393–1396.
- [15] M. I. Green, L. Hansen, “Proposal for a Cryogenic Magnetic Field Measurement System for SSC Dipole Magnets”, Super-collider 3, Springer, Boston MA, 1991. doi:10.1007/978-1-4615-3746-5\_24
- [16] D. Trbojevic *et al.*, “Alignment of the High Beta Magnets in the RHIC Interaction Regions”, in *Proc. PAC’97*, Vancouver, Canada, May 1997, paper 7P065, pp. 3651–3653.
- [17] J. DiMarco *et al.*, “Alignment of production quadrupole magnets for the LHC interaction regions”, *IEEE Trans. Appl. Supercond.*, vol. 13, no. 2, pp. 1325–1328, Jun. 2003. doi:10.1109/tasc.2003.812659
- [18] J. Billan *et al.*, “Twin rotating coils for cold magnetic measurements of 15 m long LHC dipoles”, *IEEE Trans. Appl. Supercond.*, vol. 10, no. 1, pp. 1422–1426, Mar. 2000. doi:10.1109/77.828506
- [19] P. Rogacki *et al.*, “A Rotating-Coil Scanner for the Precise Magnetic Characterization of Superconducting Accelerator Magnets at Ambient Temperature”, *IEEE Trans. Magn.*, vol. 57, no. 2, pp. 1–5, Feb. 2021. doi:10.1109/tmag.2020.3005722
- [20] J. DiMarco *et al.*, “Application of PCB and FDM Technologies to Magnetic Measurement Probe System Development”, *IEEE Trans. Appl. Supercond.*, vol. 23, no. 3, p. 9000505, Jun. 2013. doi:10.1109/tasc.2012.2236596
- [21] N. Smirnov *et al.*, “Focusing Strength Measurements of the Main Quadrupoles for the LHC”, *IEEE Trans. Appl. Supercond.*, vol. 16, no. 2, pp. 261–264, Jun. 2006. doi:10.1109/tasc.2006.871218
- [22] S. I. Bermudez *et al.*, “Progress in the Development of the Nb3Sn MQXFB Quadrupole for the HiLumi Upgrade of the LHC”, *IEEE Trans. Appl. Supercond.*, vol. 31, no. 5, pp. 1–7, Aug. 2021. doi:10.1109/tasc.2021.3061352
- [23] S. I. Bermudez *et al.*, “Status of the MQXFB Nb3Sn Quadrupoles for the HL-LHC”, *IEEE Trans. Appl. Supercond.*, vol. 33, no. 5, pp. 1–9, Aug. 2023. doi:10.1109/tasc.2023.3237503
- [24] N. Lusa *et al.*, “Towards MQXFB Series Coils”, *IEEE Trans. Appl. Supercond.*, vol. 34, no. 5, pp. 1–8, Aug. 2024. doi:10.1109/tasc.2024.3360928
- [25] S. Izquierdo Bermudez *et al.*, “Second-Generation Coil Design of the Nb3Sn low- $\beta$  Quadrupole for the High Luminosity LHC”, *IEEE Trans. Appl. Supercond.*, vol. 26, no. 4, pp. 1–5, Jun. 2016. doi:10.1109/tasc.2016.2519002